Syntheses and Properties of New Layered Alkali-Metal/Ammonium Vanadium(V) Methylphosphonates: $M(VO_2)_3(PO_3CH_3)_2$ (M = NH_4, K, Rb, Tl). Single-Crystal Structures of $K(VO_2)_3(PO_3CH_3)_2$ and $NH_4(VO_2)_3(PO_3CH_3)_2$

William T. A. Harrison,† Laurie L. Dussack, and Allan J. Jacobson*

Department of Chemistry, University of Houston, Houston, Texas 77204-5641

Received September 8, 1995[⊗]

The hydrothermal syntheses of a family of new alkali-metal/ammonium vanadium(V) methylphosphonates, $M(VO_2)_3(PO_3CH_3)_2$ (M = K, NH_4, Rb, Tl), are described. The crystal structures of $K(VO_2)_3(PO_3CH_3)_2$ and $NH_4(VO_2)_3(PO_3CH_3)_2$ have been determined from single-crystal X-ray data. Crystal data: $K(VO_2)_3(PO_3CH_3)_2$, M_r = 475.93, trigonal, *R*32 (No. 155), a = 7.139(3) Å, c = 19.109(5) Å, Z = 3; $NH_4(VO_2)_3(PO_3CH_3)_2$, M_r = 454.87, trigonal, *R*32 (No. 155), a = 7.150(3) Å, c = 19.459(5) Å, Z = 3. These isostructural, noncentrosymmetric phases are built up from hexagonal tungsten oxide (HTO) like sheets of vertex-sharing VO_6 octahedra, capped on both sides of the V/O sheets by PCH_3 entities (as $[PO_3CH_3]^{2-}$ methylphosphonate groups). In both phases, the vanadium octahedra display a distinctive two short + two intermediate + two long V−O bond distance distribution within the VO_6 unit. Interlayer potassium or ammonium cations provide charge balance for the anionic $(VO_2)_3(PO_3CH_3)_2$ sheets. Powder X-ray, TGA, IR, and Raman data for these phases are reported and discussed. The structures of $K(VO_2)_3(PO_3CH_3)_2$ and $NH_4(VO_2)_3(PO_3CH_3)_2$ are compared and contrasted with related layered phases based on the HTO motif.

Introduction

We recently reported the hydrothermal syntheses, crystal structures, and properties of a number of new layered materials[1−6] based on the hexagonal tungsten oxide (HTO) 3-ring/6-ring motif of corner-sharing octahedra.[7]

$NH_4(VO_2)_3(SeO_3)_2$[1] and $K(VO_2)_3(SeO_3)_2$[2] are the first layered-HTO type phases containing vanadium (V^V) as the octahedral cation. In these isostructural materials, 3-rings of apical oxygen atoms on both sides of the infinite vanadium/oxygen layers are capped by selenium atoms (as pyramidal $[SeO_3]^{2-}$ selenite groups), leading to infinite, anionic sheets of stoichiometry $[(VO_2)_3(SeO_3)_2]^-$. The isostructural $(NH_4)_2(MoO_3)_3SeO_3$,[3a] $Cs_2(MoO_3)_3SeO_3$,[3a] $Rb_2(MoO_3)_3SeO_3$,[3b] $Tl_2(MoO_3)_3SeO_3$,[3b] $(NH_4)_2(WO_3)_3SeO_3$,[4] and $Cs_2(WO_3)_3SeO_3$[4] contain similar, HTO-type vertex-linked MoO_6 or WO_6 layers (Mo^{VI} or W^{VI}) but are only capped by Se atoms on one side of the metal/oxygen octahedral sheets (sheet stoichiometry $[(MO_3)_3SeO_3]^{2-}$, M = Mo, W). The univalent cations provide interlayer charge balancing in all these materials.

When a source of methylphosphonate ($[PO_3CH_3]^{2-}$) anion replaces selenite in the hydrothermal syntheses, layered molybdenum(VI) and tungsten(VI) methylphosphonates are formed, as $M_2(MoO_3)_3PO_3CH_3$ (M = Rb, Cs)[5] and $M_2(WO_3)_3PO_3CH_3$ (M = NH_4, Rb, Cs).[6] These isostructural phases are also based on HTO octahedral layers, and as for corresponding molybdenum and tungsten selenites, the methylphosphonate capping occurs on only one side of the metal/oxygen sheets.

The highly anisotropic, layered structures of these HTO-type phases result in unusual octahedral metal coordination environments in these materials. In the vanadium(V)-containing systems,[1,2] the V atom is displaced from the geometric center of its six oxygen atom neighbors toward an octahedral *edge*, resulting in two short, two intermediate-length, and two long V−O bonds within the VO_6 unit. Conversely, in most of the Mo and W phases,[3−6] the metal atom is locally displaced toward an octahedral *face*, resulting in a three short + three long M−O bond distance distribution (M = Mo, W) within the MoO_6 or WO_6 unit.

In this paper we describe the hydrothermal syntheses, crystal structures, and properties of the isostructural materials $M(VO_2)_3(PO_3CH_3)_2$ (M = K, NH_4, Rb, Tl). They are built up from HTO vanadium/oxygen layers doubly capped by methylphosphonate groups. Other vanadium alkylphosphonate phases including $VO(PO_3CH_3)\cdot 1.5H_2O$[8] and novel oxovanadium diphosphonates[9] have quite different structures as compared to those of the new $M(VO_2)_3(PO_3CH_3)_2$ phases reported here.

Experimental Section

Syntheses. $K(VO_2)_3(PO_3CH_3)_2$ was hydrothermally prepared from a mixture of 0.304 g of K_2CO_3 (4.4 mmol of K), 0.40 g of V_2O_5 (4.4 mmol of V), and 1.267 g of $CH_3PO_3H_2$ (13.2 mmol of P), diluted in 10 mL of deionized water (K:V:P molar ratio = 1:1:3). The reactants were sealed in a Teflon-lined, 23-mL-capacity hydrothermal bomb and heated to 170 °C for 4 days. On cooling, product recovery by vacuum

† Present address: Department of Chemistry, University of Western Australia, Nedlands, WA 6907, Australia.

⊗ Abstract published in *Advance ACS Abstracts,* February 1, 1996.

(1) Vaughey, J. T.; Harrison, W. T. A.; Dussack, L. L.; Jacobson, A. J. *Inorg. Chem.* **1994**, *33*, 4370.
(2) Harrison, W. T. A.; Dussack, L. L.; Jacobson, A. J. *Acta Crystallogr.*, in press.
(3) (a) Harrison, W. T. A.; Dussack, L. L.; Jacobson, A. J. *Inorg. Chem.* **1994**, *33*, 6043. (b) Dussack, L. L.; Harrison, W. T. A.; Jacobson, A. J. *Mater. Res. Bull.*, in press.
(4) Harrison, W. T. A.; Dussack, L. L.; Vogt, T.; Jacobson, A. J. *J. Solid State Chem.* **1995**, *120*, 112.
(5) Harrison, W. T. A.; Dussack, L. L.; Jacobson, A. J. *Inorg. Chem.* **1995**, *34*, 4774.
(6) Harrison, W. T. A.; Dussack, L. L.; Vaughey, J. T.; Jacobson, A. J. *J. Mater. Chem.*, in press.
(7) Tournoux, M.; Ganne, M.; Piffard, Y. *J. Solid State Chem.* **1992**, *96*, 141.
(8) (a) Huan, G.; Johnson, J. W.; Brody, J. F.; Goshorn, D. P.; Jacobson, A. J. *Mater. Chem. Phys.* **1993**, *35*, 199. (b) Guliants, V. V.; Benziger, J. B.; Sundaresan, S.; Wachs, I. E.; Jehng, J.-M. *Chem. Mater.* **1995**, *7*, 1493.
(9) Soghomonian, V.; Chen, Q.; Haushalter, R. C.; Zubieta, J. *Angew. Chem., Int. Ed. Engl.* **1995**, *34*, 223 and included references.

0020-1669/96/1335-1461$12.00/0

filtration (final filtrate pH = 2.0) yielded dark forest green rhombohedral single crystals (to 0.5 mm) and powder of $K(VO_2)_3(PO_3CH_3)_2$ in 69% yield, relative to vanadium. The reaction is sensitive to temperature; the same reaction carried out at 180 °C resulted in a mixture of $K(VO_2)_3(PO_3CH_3)_2$ powder and $VO(PO_3CH_3)\cdot H_2O$.[8] Reactions at a 1:1:2 starting ratio of K:V:P led to pure $K(VO_2)_3(PO_3CH_3)_2$, while reactions starting from 1:1:<2 K:V:P led to mixtures of $K(VO_2)_3(PO_3CH_3)_2$ and $K_2V_8O_{21}$[10] (identification based on powder X-ray data). Hydrothermal reactions starting from the stoichiometric 1:3:2 K:V:P ratio of the desired product did not lead to the formation of any $K(VO_2)_3(PO_3CH_3)_2$ under the conditions used here.

Pure $NH_4(VO_2)_3(PO_3CH_3)_2$ was prepared in 90% yield (relative to vanadium) from 0.6 g of NH_4VO_3 (5.13 mmol of V) and 0.985 g of $CH_3PO_3H_2$ (10.26 mol of P), by means of a similar hydrothermal reaction (starting NH_4:V:P ratio = 1:1:2) carried out at 170 °C. Dark forest green rhombohedral crystals (to 0.2 mm) and powder of $NH_4(VO_2)_3(PO_3CH_3)_2$ were recovered as before (yield relative to V = 90%, final filtrate pH = 2.4). Similar reactions starting from a 1:1 ratio of V to P led to a reddish-brown powder of $(NH_4)_2V_6O_{16}$[11] (identified by X-ray powder measurements). Reactions (160 °C, 5 days) starting from a higher initial pH (raised to 3.8 with NH_4OH solution) led to a yellow filtrate and unidentified bronze fibers.

$Rb(VO_2)_3(PO_3CH_3)_2$ was hydrothermally prepared in 98% yield (relative to V) from a 5-day reaction at 180 °C: 0.508 g of Rb_2CO_3 (4.4 mmol Rb), 0.40 g of V_2O_5 (4.4 mmol V), and 0.845 g of $CH_3PO_3H_2$ (8.8 mmol of P) were mixed with 10 mL of water. After product recovery, the final filtrate pH was 2.45. Similar reactions at a 2:3:3 Rb:V:P starting ratio led to $Rb(VO_2)_3(PO_3CH_3)_2$ (21% yield) and unidentified orange material (final pH = 2.6). The latter phase could be removed by sonicating the solid product for 30 min in 1 M HCl. The stoichiometric 1:3:2 Rb:V:P starting mixture led to $Rb(VO_2)_3(PO_3CH_3)_2$ and an orange second phase. The best conditions for preparing $Rb(VO_2)_3(PO_3CH_3)_2$ led to dark green-black crystals of only a few microns in length.

$Tl(VO_2)_3(PO_3CH_3)_2$ (92% yield based on V) was recovered from a reaction of 1.031 g of Tl_2CO_3 (4.4 mmol of Tl), 0.40 g of V_2O_5 (4.4 mmol of V), 1.267 g of $CH_3PO_3H_2$ (13.2 mmol of P), and 10 mL of H_2O. The final pH of the hydrothermal reaction (160 °C, 5 days) was 1.95, and small, dark forest green crystals (to <0.1 mm) of $Tl(VO_2)_3(PO_3CH_3)_2$ were recovered by vacuum filtration. Reactions from a 1:1:2 Tl:V:P starting ratio led to red-orange crystals of TlV_3O_8[12] and a golden brown solid.

X-ray Powder Measurements. Diffraction data for crushed samples of the various vanadium methylphosphonates (color: very dark blackish green) were recorded on a Scintag XDS 2000 automated powder diffractometer [Cu Kα radiation, λ = 1.541 78 Å, T = 25(2) °C]. A software "stripping" and peak-fitting routine established peak positions relative to the Cu Kα_1 (λ = 1.540 56 Å) wavelength. All the patterns could be indexed on rhombohedrally-centered hexagonal unit cells (Tables 1−4). These ~7.2 × 19−19.5 Å rhombohedral unit cells suggested a close structural relationship to the layered alkali-metal/ammonium molybdenum and tungsten methylphosphonates reported earlier.[5,6]

Physical/Spectroscopic Measurements. Thermogravimetric data for the tital compounds were collected on a DuPont 9900 TG analyzer. The samples were heated at a ramp rate of 5 °C/min under flowing oxygen. The recovered post-TGA residues were characterized by powder X-ray methods. Infrared data were collected from 4000 to 400 cm^{-1} using a Galaxy FTIR 5000 series spectrometer (KBr pellet method). Raman data (KBr pellet) were collected using a coherent K-2 Kr^+ ion laser excited at 514 nm. Counts were accumulated at 1 s intervals for every two wavenumbers over the range 100−1700 cm^{-1} (Spex 1403 double monochromator/Hamamatsu 928 photomultiplier detection system).

Crystal Structure Determinations. The crystal structures of $K(VO_2)_3(PO_3CH_3)_2$ and $NH_4(VO_2)_3(PO_3CH_3)_2$ were determined by single-crystal X-ray methods: for $K(VO_2)_3(PO_3CH_3)_2$, a brilliantly-faceted, slightly translucent, blackish-green rhomb (dimensions ~0.1 × 0.1 × 0.1 mm) was mounted on a thin glass fiber with cyanoacrylate glue, and room-temperature [25(2) °C] intensity data were collected on an Enraf-Nonius CAD4 automated four-circle diffractometer (graphite-monochromated Mo Kα radiation, λ = 0.710 73 Å). Pre-

Table 1. X-ray Powder Data for $K(VO_2)_3(PO_3CH_3)_2$

Rhombohedral: a = 7.137(2) Å, c = 19.091(4) Å, V = 842.2 Å^3

h	k	l	d_{obs} (Å)	d_{calc} (Å)	I_{rel}[a]
0	0	3	6.364	6.364	73
1	0	1	5.882	5.881	50
0	1	2	5.188	5.188	54
1	1	0	3.565	3.569	15
0	0	6	3.181	3.182	28
1	1	3	3.111	3.113	100
0	2	1	3.050	3.051	33
2	0	2	2.938	2.940	18
0	2	4	2.594	2.594	19
1	0	7	2.500	2.495	59
1	1	6	2.375	2.375	8
2	1	1	2.317	2.319	7
1	2	2	2.271	2.269	7
0	1	8	2.226	2.226	6
0	0	9	2.121	2.121	40
2	1	4	2.099	2.099	7
3	0	3	1.961	1.960	21

[a] $I_{rel} = 100I/I_{max}$.

Table 2. X-ray Powder Data for $NH_4(VO_2)_3(PO_3CH_3)_2$

Rhombohedral: a = 7.1435(7) Å, c = 19.441(3) Å, V = 859.1 Å^3

h	k	l	d_{obs} (Å)	d_{calc} (Å)	I_{rel}[a]
0	0	3	6.481	6.480	52
1	0	1	5.893	5.895	23
0	1	2	5.220	5.219	100
1	1	0	3.570	3.572	12
0	0	6	3.239	3.240	10
1	1	3	3.127	3.128	88
0	2	1	3.054	3.055	62
2	0	2	2.946	2.948	7
0	2	4	2.610	2.610	11
1	0	7	2.534	2.534	21
1	1	6	2.400	2.400	10
2	1	1	2.321	2.322	6
1	2	2	2.274	2.273	4
0	0	9	2.160	2.160	17

[a] $I_{rel} = 100I/I_{max}$.

Table 3. X-ray Powder Data for $Rb(VO_2)_3(PO_3CH_3)_2$

Rhombohedral: a = 7.1576(7) Å, c = 19.409(2) Å, V = 861.1 Å^3

h	k	l	d_{obs} (Å)	d_{calc} (Å)	I_{rel}[a]
0	0	3	6.470	6.470	15
1	0	1	5.906	5.905	63
0	1	2	5.223	5.224	20
1	0	4	3.822	3.821	9
1	1	0	3.576	3.579	21
0	1	5	3.288	3.290	2
0	0	6	3.233	3.235	14
1	1	3	3.130	3.132	100
0	2	1	3.059	3.061	12
2	0	2	2.951	2.952	14
0	2	4	2.612	2.612	19
1	0	7	2.531	2.531	29
1	1	6	2.400	2.400	2
2	1	1	2.326	2.326	7
0	1	8	2.259	2.259	6
0	0	9	2.157	2.157	6
2	1	4	2.110	2.110	6
3	0	3	1.969	1.969	20
2	0	8	1.911	1.910	5
1	1	9	1.847	1.847	2
2	1	7	1.790	1.790	17

[a] $I_{rel} = 100I/I_{max}$.

(10) JCPDS Powder Diffraction File, Card 24-0906.
(11) JCPDS Powder Diffraction File, Card 22-1046.
(12) JCPDS Powder Diffraction File, Card 32-1347.

Table 4. X-ray Powder Data for $Tl(VO_2)_3(PO_3CH_3)_2$

Rhombohedral: $a = 7.1602(5)$ Å, $c = 19.363(2)$ Å, $V = 859.7$ Å^3

h	k	l	d_{obs} (Å)	d_{calc} (Å)	I_{rel}[a]
1	0	1	5.906	5.906	85
1	0	4	3.816	3.816	23
1	1	0	3.580	3.580	30
0	1	5	3.283	3.285	13
0	0	6	3.225	3.227	15
1	1	3	3.130	3.131	100
2	0	2	2.952	2.953	22
0	2	4	2.610	2.611	22
1	0	7	2.526	2.526	30
2	0	5	2.420	2.420	7
1	1	6	2.397	2.397	6
2	1	1	2.327	2.327	13
1	2	2	2.278	2.278	13
0	1	8	2.255	2.255	8
2	1	4	2.109	2.110	10
3	0	0	2.066	2.067	4
1	2	5	2.006	2.005	3
3	0	3	1.969	1.969	19
2	0	8	1.908	1.908	6
1	1	9	1.844	1.844	5
2	2	0	1.790	1.790	15

[a] $I_{rel} = 100I/I_{max}$.

liminary measurements indicated a rhombohedrally-centered lattice, in agreement with the powder X-ray measurements, and 659 data ($0 \rightarrow h$, $0 \rightarrow k$, $-l \rightarrow l$) were scanned for $1° < 2\theta < 60°$.

During data reduction, an absorption correction based on ψ scans (minimum 1.16, maximum 1.35) was applied to the data. The systematic absence condition ($hkil$: $-h + k + l \neq 3n$) was consistent with space groups $R3$, $R\bar{3}$, $R32$, $R3m$, and $R\bar{3}m$. Initial data merges indicated that Laue class $3\bar{m}1$ was probably the correct one [$R_{Int} = 4.58\%$, 337 merged data, 296 observed data with $I > 3\sigma(I)$].

The crystal-structure model of $K(VO_2)_3(PO_3CH_3)_2$ was initially developed in space group $R3$, with atomic models based on the related singly-capped $M_2(MoO_3)_3PO_3CH_3$ phases[5] (software CRYSTALS;[13] complex, neutral-atom scattering factors from ref 14). Location of additional atomic sites from difference Fourier maps indicated that both sides of the vanadium/oxygen layers were capped by methylphosphonate groups in $K(VO_2)_3(PO_3CH_3)_2$. A symmetry check (program MISSYM[15]) indicated that space group $R32$ was the best one to describe the atomic positions in $K(VO_2)_3(PO_3CH_3)_2$. Refinement in this space group was successful, and other space groups were rejected from further consideration. The hydrogen atom in $K(VO_2)_3(PO_3CH_3)_2$ was located from a difference Fourier synthesis, and its positional parameters were refined without constraints.

The data collection and refinement procedures for $NH_4(VO_2)_3(PO_3CH_3)_2$ were essentially identical to those of $K(VO_2)_3(PO_3CH_3)_2$: blackish-green rhomb; $0.2 \times 0.2 \times 0.3$ mm; rhombohedral; $1° < 2\theta < 60°$; 678 data ($0 \rightarrow h$, $0 \rightarrow k$, $-l \rightarrow l$); space group $R32$; absorption correction from ψ scans (minimum 1.55, maximum 1.81); $R_{Int} = 1.05\%$; 343 merged data; 322 observed data [$I > 3\sigma(I)$]. The $K(VO_2)_3(PO_3CH_3)_2$ atomic coordinates were used as a starting model (N substituting for K) and refined successfully. The C−H proton was located from difference maps and refined without constraints. The NH_4 protons could not be located or unambiguously placed geometrically.

Crystallographic data for $K(VO_2)_3(PO_3CH_3)_2$ and $NH_4(VO_2)_3(PO_3CH_3)_2$ are summarized in Table 5. Anisotropic thermal parameters are available as Supporting Information.

Results

Crystal Structures. Final atomic positional and equivalent isotropic thermal parameters for $K(VO_2)_3(PO_3CH_3)_2$ are listed in Table 6, with selected bond distance/angle data in Table 7. Comparable data for $NH_4(VO_2)_3(PO_3CH_3)_2$ are listed in Tables 8 and 9.

Table 5. Crystallographic Parameters

	$K(VO_2)_3(PO_3CH_3)_2$	$NH_4(VO_2)_3(PO_3CH_3)_2$
empirical formula	$V_3KP_2O_{12}C_2H_6$	$V_3P_2NO_{12}C_2H_{10}$
fw	475.93	454.87
a (Å)	7.139(3)	7.150(2)
c (Å)	19.109(5)	19.459(5)
V (Å^3)	843.4(6)	862.1(4)
Z	3	3
space group	$R32$ (No. 155)	$R32$ (No. 155)
T (°C)	25(2)	25(2)
λ(Mo Kα) (Å)	0.710 73	0.710 73
ρ_{calc} (g/cm^3)	2.81	2.63
μ(Mo Kα) (cm^{-1})	30.80	26.56
$R(F)$[a] (%)	2.83	2.93
$R_w(F)$[b] (%)	2.57	3.07

[a] $R = 100\sum||F_o| - |F_c||/\sum|F_o|$. [b] $R_w = 100[\sum w(|F_o| - |F_c|)^2/\sum w|F_o|^2]^{1/2}$, with $w_i = 1/\sigma(F_i)^2$.

Table 6. Atomic Positional/Thermal Parameters for $K(VO_2)_3(PO_3CH_3)_2$

atom	x	y	z	U_{eq}[a] (Å^2)
K(1)	0	0	$^1/_2$	0.0281
V(1)	0.5464(1)	0	0	0.0099
P(1)	$^2/_3$	$^1/_3$	0.12102(9)	0.0074
O(1)	0.5472(6)	0.0980(5)	0.0959(1)	0.0096
O(2)	0.5867(5)	−0.2031(6)	0.0201(1)	0.0104
C(1)	$^2/_3$	$^1/_3$	0.2138(4)	0.0106
H(1)	0.146(8)	0.07(1)	0.104(2)	0.02[b]

[a] $U_{eq} = (U_1U_2U_3)^{1/3}$. [b] U_{iso} (not refined).

Table 7. Bond Distances (Å)/Angles (deg) for $K(VO_2)_3(PO_3CH_3)_2$

K(1)−O(1) × 6	2.990(3)	V(1)−O(1) × 2	1.961(2)
V(1)−O(2) × 2	1.658(4)	V(1)−O(2) × 2	2.174(4)
P(1)−O(1) × 3	1.532(3)	P(1)−C(1)	1.773(7)
C(1)−H(1) × 3	0.95(5)		
O(1)−K(1)−O(1)	101.15(6)	O(1)−K(1)−O(1)	79.2(1)
O(1)−K(1)−O(1)	179.5(2)	O(1)−K(1)−O(1)	78.5(1)
O(1)−V(1)−O(1)	159.8(2)	O(1)−V(1)−O(2)	97.2(1)
O(1)−V(1)−O(2)	95.1(1)	O(1)−V(1)−O(2)	83.3(1)
O(1)−V(1)−O(2)	81.0(1)	O(2)−V(1)−O(2)	89.1(2)
O(2)−V(1)−O(2)	104.7(2)	O(2)−V(1)−O(2)	166.20(7)
O(2)−V(1)−O(2)	77.1(2)	O(1)−P(1)−O(1)	110.7(1)
O(1)−P(1)−C(1)	108.2(1)	V(1)−O(1)−P(1)	125.8(2)
V(1)−O(2)−V(1)	140.9(2)	P(1)−C(1)−H(1)	108(3)
H(1)−C(1)−H(1)	111(3)		

Table 8. Atomic Positional Parameters for $NH_4(VO_2)_3(PO_3CH_3)_2$

atom	x	y	z	U_{eq}[a] (Å^2)
N(1)	0	0	$^1/_2$	0.0153
V(1)	0.5468(2)	0	0	0.0098
P(1)	$^2/_3$	$^1/_3$	0.1191(1)	0.0075
O(1)	0.5465(6)	0.0958(5)	0.0943(1)	0.0096
O(2)	0.5862(5)	−0.2026(6)	0.0200(1)	0.0105
C(1)	$^2/_3$	$^1/_3$	0.2104(4)	0.0130
H(1)	0.158(9)	0.06(1)	0.108(2)	0.02[b]

[a] $U_{eq} = (U_1U_2U_3)^{1/3}$. [b] U_{iso} (not refined).

$K(VO_2)_3(PO_3CH_3)_2$ and $NH_4(VO_2)_3(PO_3CH_3)_2$ are isostructural new phases built up from potassium/ammonium cations and layers of vertex-sharing VO_6 and PO_3CH_3 units, which are fused together by V−O−V′ and V−O−P bonds. A fragment of the V/P/O/CH_3 layer is shown in Figure 1, and the complete crystal structure of $K(VO_2)_3(PO_3CH_3)_2$ is illustrated in Figure 2.

Like the phases mentioned in the introduction,[1−6] $K(VO_2)_3(PO_3CH_3)_2$ and $NH_4(VO_2)_3(PO_3CH_3)_2$ are built up from hexagonal tungsten oxide[7] type layers of corner-sharing VO_6 units, as

(13) Watkin, D. J.; Carruthers, J. R.; Betteridge, P. W. *CRYSTALS User Guide*; Chemical Crystallography Laboratory, Oxford University: Oxford, U.K., 1993.
(14) Cromer, D. T. *International Tables for X-Ray Crystallography*; Kynoch Press: Birmingham, U.K., 1974; Vol. IV, Table 2.3.1.
(15) Le Page, Y. *J. Appl. Crystallogr.* **1988**, *21*, 983.

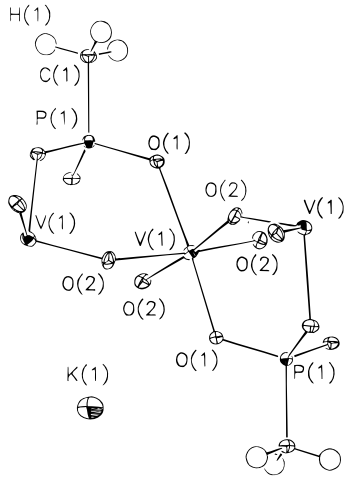

Figure 1. ORTEP view of a fragment of the $K(VO_2)_3(PO_3CH_3)_2$ structure, showing the atom-labeling scheme (50% thermal ellipsoids).

Table 9. Bond Distances (Å)/Angles (deg) for $NH_4(VO_2)_3(PO_3CH_3)_2$

N(1)−O(1) × 6	3.007(3)	V(1)−O(1) × 2	1.960(3)
V(1)−O(2) × 2	1.654(4)	V(1)−O(2) × 2	2.185(4)
P(1)−O(1) × 3	1.547(3)	P(1)−C(10	1.777(8)
C(1)−H(1) × 3	1.03(5)		
O(1)−N(1)−O(1)	99.87(6)	O(1)−N(1)−O(1)	80.4(1)
O(1)−N(1)−O(1)	179.6(2)	O(1)−N(1)−O(1)	79.8(1)
O(1)−V(1)−O(1)	159.7(3)	O(1)−V(1)−O(2)	96.6(2)
O(1)−V(1)−O(2)	95.6(1)	O(1)−V(1)−O(2)	82.9(1)
O(1)−V(1)−O(2)	81.3(1)	O(2)−V(1)−O(2)	88.8(2)
O(2)−V(1)−O(2)	105.1(2)	O(2)−V(1)−O(2)	166.10(8)
O(2)−V(1)−O(2)	77.3(2)	O(1)−P(1)−O(1)	110.8(1)
O(1)−P(1)−C(1)	108.1(1)	V(1)−O(1)−P(1)	125.3(2)
V(1)−O(2)−V(1)	140.8(2)	P(1)−C(1)−H(1)	107(3)
H(1)−C(1)−H(1)	112(3)		

shown in Figure 3. Each VO_6 unit shares four of its V−O vertices with similar neighbors; the V−O−V′ bonds form buckled layers about the *ab* plane. These V−O bonds are canted from the *ab* plane by ∼12° in both $K(VO_2)_3(PO_3CH_3)_2$ and $NH_4(VO_2)_3(PO_3CH_3)_2$. The two apical V−O bonds point approximately in the *c* direction, one above the plane and one below. 3-Rings and 6-rings of VO_6 octahedra result from this arrangement (Figure 3). These apical V−O bonds are actually canted some 20° away from the *z* direction, which forces the oxygen atoms of the 3-rings closer together and allows the methylphosphonate groups to fuse with the V−O bonds and cap both sides of the vanadium/oxygen sheet. The overall sheet stoichiometry is $[(VO_2)_3(PO_3CH_3)_2]^{2-}$, with charge compensation provided by interlayer potassium or ammonium cations.

In both $K(VO_2)_3(PO_3CH_3)_2$ and $NH_4(VO_2)_3(PO_3CH_3)_2$, the VO_6 octahedron is significantly distorted from octahedral regularity. The vanadium atom (site symmetry .2) is displaced from the center of its six O atom neighbors [2 × O(1), 4 × O(2)] toward an octahedral edge consisting of two of the O(2) atoms ("local 110" distortion; Figure 4). This distortion, by 0.34 Å from the geometric center of the VO_6 octahedron for $K(VO_2)_3(PO_3CH_3)_2$ and by 0.35 Å for $NH_4(VO_2)_3(PO_3CH_3)_2$, is exactly along the [100] crystallographic direction. It results in two short (d < 1.7 Å) V−O(2) bonds in *cis* configuration, both of which are each *trans* to a long (d > 2.1 Å) V−O(2) link. The V−O(1) bonds are of intermediate length between these two extremes (Tables 7 and 9). Bond valence sum (BVS) calculations[16] assign a BVS of ∼1.5 to the short V−O(2) bonds, similar to values determined for terminal V═O "vanadyl" double bonds in other V^V-containing systems.[17] The overall vanadium BVS values (5.00 for $K(VO_2)_3(PO_3CH_3)_2$; 5.01 for $NH_4(VO_2)_3(PO_3CH_3)_2$) are commensurate with the expected value of 5.00 for vanadium(V), despite the unusual V atom coordination in these phases (see below). For both phases, the single distinct inter V atom link [*via* O(2)] consists of a short (<1.7 Å) and a long (>2.1 Å) V−O bond, *i.e.* V═O−V′ and V−O═V′ links (Figure 5).

The methylphosphonate group has typical geometrical parameters[18] in both $K(VO_2)_3(PO_3CH_3)_2$ and $NH_4(VO_2)_3(PO_3CH_3)_2$ (Tables 7 and 9). The P and C atoms are on a 3-fold

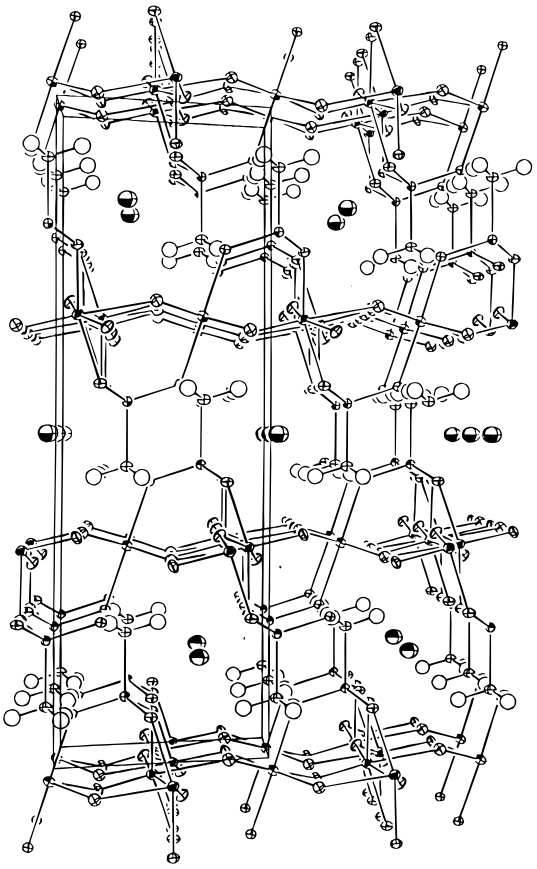

Figure 2. Unit-cell packing of $K(VO_2)_3(PO_3CH_3)_2$, viewed down [010], showing the sheet structure (K−O contacts not shown).

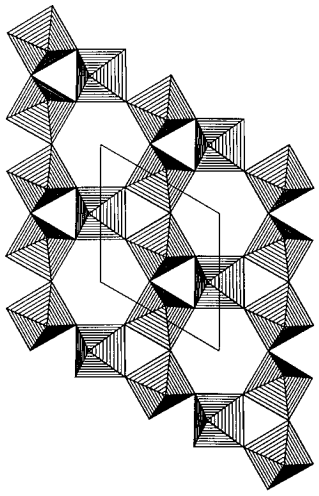

Figure 3. Polyhedral plot of a hexagonal tungsten oxide like 3-ring/6-ring layer of vertex-sharing octahedra, viewed down [001].

(16) Brese, N. E.; O'Keeffe, M. *Acta Crystallogr.* **1991**, *B47*, 192.

(17) Gopal, R.; Calvo, C. *J. Solid State Chem.* **1972**, *5*, 432.

(18) Stalick, J. K.; Quicksall, C. O. *Inorg. Chem.* **1976**, *15*, 1577.

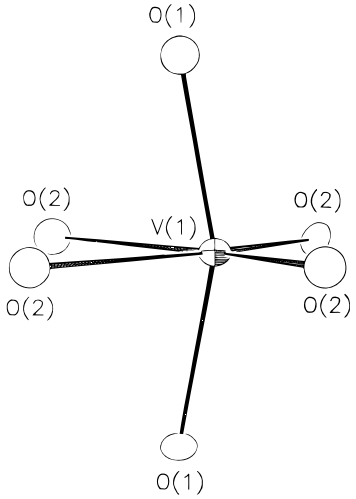

Figure 4. Detail of the VO_6 octahedron in $K(VO_2)_3(PO_3CH_3)_2$, showing the local V atom displacement toward an octahedral edge.

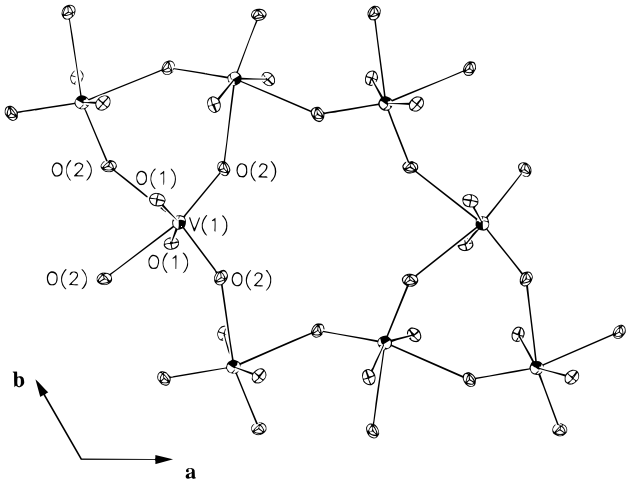

Figure 5. View down [001] of the in-plane linkage of VO_6 octahedra in $K(VO_2)_3(PO_3CH_3)_2$.

axis, and three equivalent P(1)−O(1) bonds result, each of which bridges to a different VO_6 unit. The methyl group hydrogen atom in $K(VO_2)_3(PO_3CH_3)_2$ is almost exactly staggered (H−C−P−O torsion angle = 177°) with respect to the adjacent PO_3 moiety and is separated by approximately 3 Å from nonbonding oxygen atoms in the adjacent $(VO_2)_3(PO_3CH_3)_2$ sheet.

The single crystallographically-distinct cation site (site symmetry 32) is found in the interlayer region for these phases. In $K(VO_2)_3(PO_3CH_3)_2$, K(1) is six-coordinated (Figure 6) to nearby oxygen atoms and forms a distorted octahedron. The K atom is essentially bound to a pair of oxygen atom 3-rings in the two adjacent $(VO_2)_3(PO_3CH_3)_2$ layers. The bond valence sum for K(1) is only 0.59, compared to an ideal value of 1.00, suggesting that these layered structures are not crucially defined by the bonding requirements of the univalent cation. The ammonium cation [atom N(1)] in $NH_4(VO_2)_3(PO_3CH_3)_2$ occupies the same site as the K species in $K(VO_2)_3(PO_3CH_3)_2$. The N···O contact distance in $NH_4(VO_2)_3(PO_3CH_3)_2$ is slightly larger than the K−O distance in $K(VO_2)_3(PO_3CH_3)_2$ (Tables 7 and 9). This is perhaps reflected in the larger *c* unit cell dimension in the ammonium phase, compared to the potassium material. No information regarding possible ammonium H-bonding interactions in $NH_4(VO_2)_3(PO_3CH_3)_2$ could be extracted from the X-ray data. The equivalent isotropic thermal factor for K(1) in $K(VO_2)_3(PO_3CH_3)_2$ is somewhat larger than that for the N(1) species in $NH_4(VO_2)_3(PO_3CH_3)_2$, suggesting that

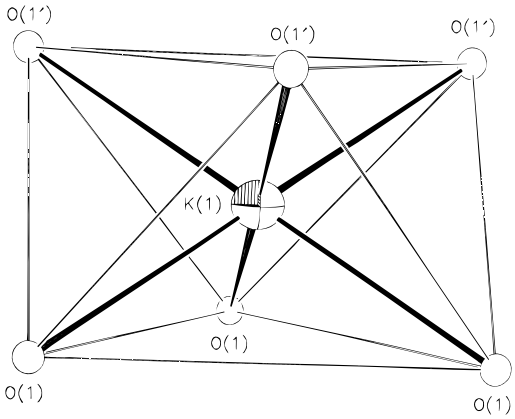

Figure 6. K(1) coordination in $K(VO_2)_3(PO_3CH_3)_2$. Nonbonding O···O contacts are indicated by thin lines: The O(1) species belong to one $(VO_2)_3(PO_3CH_3)_2$ layer; the O(1′), to the adjacent layer (d[O(1)···O(1)] = 4.62 Å, d[O(1)···O(1′)] = 3.78 and 3.81 Å).

the potassium cation is somewhat undersized for its six-coordinate site in this material.

The $(VO_2)_3(PO_3CH_3)_2$ layers in these $M(VO_2)_3(PO_3CH_3)_2$ phases make an ABCABC... repeat motif in the crystallographic *z*-direction. Adjacent layers are staggered, such that every methylphosphonate group points toward a 6-ring window in the adjacent $(VO_2)_3(PO_3CH_3)_2$ layer. Thus, there are no pseudo-one-dimensional channels in this structure, comparable to the infinite [001] channels found in hexagonal-WO_3 and M_xWO_3 (M = Rb, K, NH_4, ...) type materials.[19]

Thermogravimetric Data. TGA for $K(VO_2)_3(PO_3CH_3)_2$ heated to 500 °C in oxygen showed a two-step weight loss of 6.9% from 390 to 450 °C, followed by a sharp weight gain of 2.5%. The brown, glassy residue is amorphous. $NH_4(VO_2)_3(PO_3CH_3)_2$ (heated to 600 °C) showed a gradual two-step 12.9% weight loss from 300 to 480 °C, followed by a rapid weight gain (3.8%) by 520 °C. The yellow post-TGA residue consists of β-$VOPO_4$[20] and other phases. The total nominal weight loss for removal of all N, C, H, and water from $NH_4(VO_2)_3(PO_3CH_3)_2$ is 12.3%. TGA for $Rb(VO_2)_3(PO_3CH_3)_2$ showed a rapid weight loss of 8.4% between 410 and 420 °C, followed by a weight gain of 4.2% to 500 °C. $Tl(VO_2)_3(PO_3CH_3)_2$ heated to 550 °C showed a clean, two-step weight loss of 6.5% between 370 and 390 °C, followed by a gradual weight gain of 3.8%. The brown residue is amorphous.

Interpretation of these data is complicated by the uncertain decomposition pathways and the glassy and amorphous post-TGA residues. The phenomenon of weight loss followed by weight gain may be attributed to partial reduction of vanadium(V) during the decomposition process, followed by reoxidation. We note that these phases are thermally stable to at least 300 °C for $NH_4(VO_2)_3(PO_3CH_3)_2$ and in the 370−410 °C range for the other cations.

Spectroscopic Data. The IR spectra (Figure 7) for the $M(VO_2)_3(PO_3CH_3)_2$ phases do not show any bands attributable to water molecule vibrations. All four phases show very similar C−H, V−O, P−O, and P−C stretches (bands identified by analogy with previously known phases[1−6,21,22]). IR for $NH_4(VO_2)_3(PO_3CH_3)_2$ also shows bands attributable to NH_4 modes at 3173, 3040, and 1414 cm^{-1}. The strong band at ~810

(19) Labbe, P. H.; Goreaud, M.; Raveau, B.; Monier, J. C. *Acta Crystallogr.* **1978**, *B34*, 1433.
(20) JCPDS Powder Diffraction File, Card 27-948.
(21) Kwak, W.; Pope, M. T.; Scully, T. F. *J. Am. Chem. Soc.* **1975**, *97*, 5735.
(22) Nakamoto, K. *Infrared and Raman Spectra of Inorganic and Coordination Compounds*, 9th ed.; Wiley-Interscience: New York, 1986.

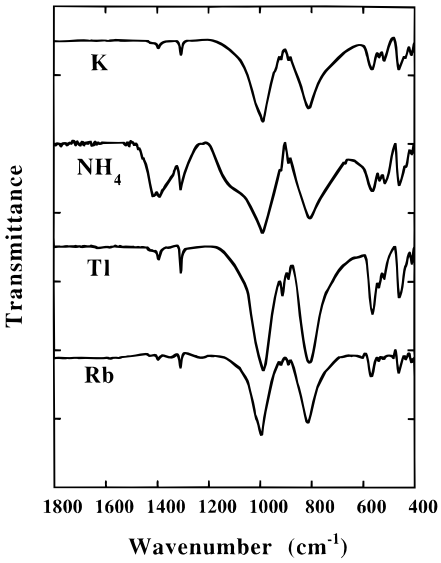

Figure 7. IR spectra of $M(VO_2)_3(PO_3CH_3)_2$ phases.

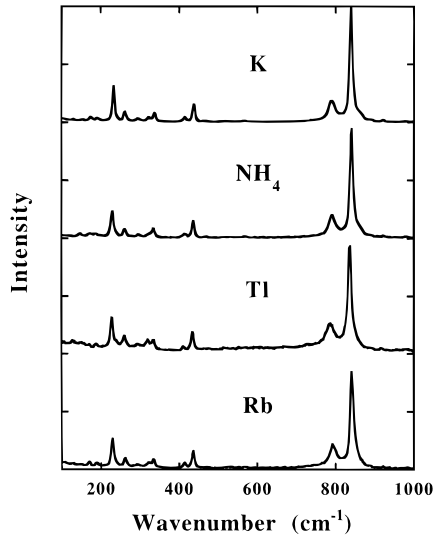

Figure 8. Raman spectra of $M(VO_2)_3(PO_3CH_3)_2$ phases.

Table 10. Spectroscopic Data (cm^{-1}) for $M(VO_2)_3(PO_3CH_3)_2$ Phases[a]

phase	ν(P−O)	ν(V−O)	ν(C−H)	ν(P−C)
$K(VO_2)_3(PO_3CH_3)_2$	987/789	808/840	2945	1309
$NH_4(VO_2)_3(PO_3CH_3)_2$	991/792	810/841	2938	1308
$Rb(VO_2)_3(PO_3CH_3)_2$	988/787	808/838	2938	1308
$Tl(VO_2)_3(PO_3CH_3)_2$	995/794	814/843	2940	1310

[a] Where two values are given, the first refers to IR and the second to Raman (see text).

cm^{-1} is identified as a VO stretching vibration (distorted octahedral VO_6 coordination) by comparison with the IR spectra of $NH_4(VO_2)_3(SeO_3)_2$[1] and $K(VO_2)_3(SeO_3)_2$.[2] The methyl group is identified by bands at ∼2940 cm^{-1} (stretching) and ∼1395 cm^{-1} (bending). The strong, broad peak at ∼990 cm^{-1} is associated with methylphosphonate P−O modes, and the weak, sharp peak at 1309 cm^{-1} is typical for a P−C alkylphosphonate stretch.[20] This P−C mode was observed at similar frequencies in the tungsten methylphosphonates.[6] The main IR absorption frequencies for the individual $M(VO_2)_3(PO_3CH_3)_2$ phases are listed in Table 10.

The Raman data for the four samples are generally similar (Figure 8; Table 10). Strong, sharp bands corresponding to VO stretching modes are seen in the 837−840 cm^{-1} range. The P−O symmetric stretch is apparent at ∼790 cm^{-1} and corresponds with similar features seen in the Raman spectra for the $M_2(MoO_3)_3PO_3CH_3$ phases.[5] This band is not apparent in the IR spectra because of overlap with the strong VO modes at ∼810 cm^{-1}. The $NH_4(VO_2)_3(PO_3CH_3)_2$ and $Tl(VO_2)_3(PO_3CH_3)_2$ phases showed some color change in the 514 nm laser beam; experiments carried out at 406 nm led to sample decomposition.

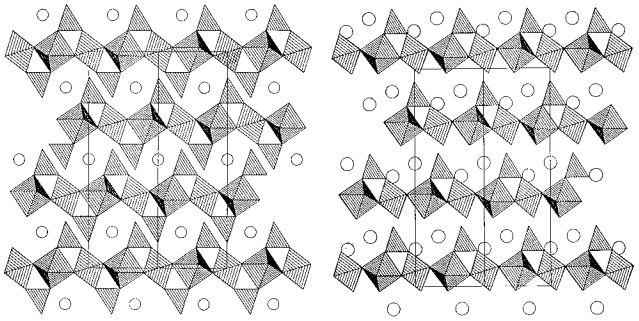

Figure 9. Polyhedral plots of (left) the $M(VO_2)_3(PO_3CH_3)_2$ and (right) the $M_2(MoO_3)_3PO_3CH_3$ structures, showing the doubly-capped octahedral layers in the vanadium phases and the singly-capped layers in the molybdenum phases. Interlayer cations are represented by plain circles.

Discussion

A new family of layered alkali-metal/ammonium vanadium(V) methylphosphonate phases, $M(VO_2)_3(PO_3CH_3)_2$, have been prepared and characterized for the first time. On the basis of X-ray powder patterns and physical data, they are isostructural, with slight variations in their unit-cell parameters. There are no particular correlations between interlayer cation size and individual unit-cell parameters, although the unit-cell volume systematically increases with larger cation size. The physical and spectroscopic data for these phases may be understood in relationship to their crystal structures. The single-crystal structures of $K(VO_2)_3(PO_3CH_3)_2$ and $NH_4(VO_2)_3(PO_3CH_3)_2$ are almost identical and reveal a structure based on a hexagonal tungsten oxide motif of layers of corner-sharing VO_6 groups, capped by PCH_3 (as methylphosphonate) entities on both faces of the vanadium/oxygen sheets. All the available structural evidence (BVS values, charge neutrality criterion assuming that all atomic sites are fully occupied and that the K^+/NH_4^+, O^{2-}, and $[PO_3CH_3]^{2-}$ species adopt their normal, stable valence) indicates that vanadium is present only as V^V in these materials.

Moderate-condition (T = 150−200 °C) hydrothermal synthesis, under carefully controlled conditions (especially pH), was successful in preparing these phases, following the precedent of the other HTO phases described in the Introduction. $K(VO_2)_3(PO_3CH_3)_2$ and $NH_4(VO_2)_3(PO_3CH_3)_2$ formed crystals large enough for single-crystal X-ray characterization. We note that only $Rb(VO_2)_3(PO_3CH_3)_2$, in impure form, could be hydrothermally prepared at the stoichiometric 1:3:2 M:V:P starting ratio.

The $M(VO_2)_3(PO_3CH_3)_2$ phases complement the layered vanadium, molybdenum, and tungsten HTO phases noted in the Introduction[1−6] but are not isostructural with any of them. There are three important ways to classify members of this family of phases: single or double capping of the octahedral layers; the stacking sequence perpendicular to the layers; the distortion mode of the octahedral cation. The $M(VO_2)_3(PO_3CH_3)_2$ materials are capped on both faces of the V/O sheets, like the layered vanadium selenites.[1,2] They form a three-layer repeat motif, like the singly-capped molybdenum and tungsten methylphosphonates (Figure 9).[5,6] The VO_6 octahedra in $K(VO_2)_3(PO_3CH_3)_2$ and $NH_4(VO_2)_3(PO_3CH_3)_2$ show a distinctive local distortion of the vanadium atom toward an octahedral edge.

The $M(VO_2)_3(PO_3CH_3)_2$ phases form a three-layer (ABCABC...) periodicity in the crystallographic *c* direction. The displacement of adjacent layers in the *a* and *b* directions results in the methylphosphonate groups pointing toward an unoccupied octahedral 6-ring in an adjacent $(VO_2)_3(PO_3CH_3)_2$ layer. This effect, which may be correlated with the steric effect (size) of the methylphosphonate group, was also observed in the singly-capped $M_2(MoO_3)_3PO_3CH_3$[5] and $M_2(WO_3)_3PO_3CH_3$[6] structures. The methylphosphonate adopts a normal staggered configuration in all these phases. In the molybdenum and tungsten methylphosphonate phases, there are two distinct interlayer cations; one of these occupies a site similar to those of the K(1) and N(1) species in $K(VO_2)_3(PO_3CH_3)_2$ and $NH_4(VO_2)_3(PO_3CH_3)_2$, respectively. The other cation in the Mo and W methylphosphonates occupies a 6-ring site. Because a methylphosphonate group points toward every 6-ring in $K(VO_2)_3(PO_3CH_3)_2$ and $NH_4(VO_2)_3(PO_3CH_3)_2$, this second cation site is not available in the $M(VO_2)_3(PO_3CH_3)_2$ phases.

The octahedral distortions of the VO_6 groups in $K(VO_2)_3(PO_3CH_3)_2$ and $NH_4(VO_2)_3(PO_3CH_3)_2$ are distinctive and unusual and may be visualized as local "[110]" shifts of the V atom within its oxygen atom octahedron toward an octahedral *edge*. The oxygen atom octahedra in $K(VO_2)_3(PO_3CH_3)_2$ and $NH_4(VO_2)_3(PO_3CH_3)_2$ are fairly regular, with minimum, average, and maximum *cis* O···O contacts of 2.62, 2.70, and 2.75 Å, respectively, in $K(VO_2)_3(PO_3CH_3)_2$. The resulting two short + two intermediate + two long V−O bond distance distribution (short bonds in *cis* configuration) within the VO_6 unit is also seen in the $M(VO_2)_3(SeO_3)_2$ phases.[1,2] In the $M(VO_2)_3(PO_3CH_3)_2$ phases, the vanadium atom site symmetry is .2, whereas in the selenites it is 1. The more common V^V displacement within its O atom octahedron is along a V−O bond axis, which results in one short ($d < \sim 1.7$ Å) V−O bond *trans* to a long ($d > \sim 2.1$ Å) V−O bond and four V−O bonds of intermediate length.[17] Indeed, the single, short V═O "vanadyl" bond (or $[VO]^{3+}$ group) is often regarded as characteristic of vanadium(V). However, some vanadium(V) compounds such as V_2O_5 adopt a more complex distortion mode.[1] We note that the two short + two intermediate + two long octahedral bond distance distribution is typically found for *molybdenum(VI)* compounds, although, as noted above, the HTO-type Mo^{VI} compounds[3,5] adopt a *different* three short + three long distortion mode (Mo shifts toward an octahedral *face*).

The displacement of a formal d^0 cation such as V^V in octahedral coordination may be understood in terms of a second-order Jahn−Teller effect:[23] "Spontaneous" distortion of the VO_6 group will remove (near) degeneracies in the molecular energy levels which arise from overlap of the unoccupied d orbitals of the metal species with the filled p orbitals of the oxygen atom species. The magnitude and *direction* of the cation displacement inside its octahedron are much more difficult to predict from first principles and reflect a combination of second-order electronic effects, lattice stresses, and cation−cation repulsions, as discussed recently by Kunz and Brown.[24] Detailed analysis of the VO_6 distortions in the $M(VO_2)_3(PO_3CH_3)_2$ phases requires further work. However, we note here that in-plane V···V cation−cation interactions, as constrained by 3-fold symmetry, do appear to be minimized by the local [110] VO_6 distortions observed: The four equivalent (each VO_6 group is bound to four nearest neighbor octahedra), in-plane nearest-neighbor V···V distances in $K(VO_2)_3(PO_3CH_3)_2$ are 3.62 Å. If the VO_6 groups were undistorted [V occupies a ($^1/_2$, 0, 0) site], then the equivalent V···V interaction distances would be 3.56 Å (reduction of some 1.5%). Conversely, if the V atom were nominally displaced from ($^1/_2$, 0, 0) toward one of the in-plane O(2) species, resulting in a single 1.65 Å link to O(2) *trans* to a 2.15 Å link, then four shortest V···V interactions of ~3.58 Å result. This nominal distortion would require the crystal symmetry to be lowered from *R*32 to avoid V atom disorder effects. This simple analysis takes no account of the tilting of the VO_6 octahedra due to their capping or any out-of-plane interactions with the methylphosphonate groups or interlayer cations. The effect of the cation is probably small, since the $(VO_2)_3(PO_3CH_3)_2$ geometries in $K(VO_2)_3(PO_3CH_3)_2$ and $NH_4(VO_2)_3(PO_3CH_3)_2$ are virtually identical. Other layered vanadium organophosphonates based on sheet motifs involving both V−O−V′ and V−O−P bonds have been described elsewhere.[25,26]

Conclusions

A new family of isostructural, layered, noncentrosymmetric vanadium(V) methylphosphonates, $M(VO_2)_3(PO_3CH_3)_2$ (M = K, NH_4, Rb, Tl), have been hydrothermally prepared and characterized. Their spectroscopic and physical properties are consistent with their crystal chemistry. They extend the series of other layered phases based on a hexagonal tungsten oxide motif described recently.[1−6] The layer stacking sequence in the $M(VO_2)_3(PO_3CH_3)_2$ phases may be understood in terms of minimizing interlayer steric effects, and the unusual vanadium(V) octahedral distortions in these phases may be empirically correlated with minimization of cation−cation repulsions. We are presently investigating the optical and other physical properties of these phases.

Acknowledgment. We thank Paul Meloni and Roman Czernuszewicz for assistance in collecting the Raman data. This work was funded by the National Science Foundation (Grant DMR9214804) and the Robert A. Welch Foundation (Grant E-1207).

Supporting Information Available: Tables of anisotropic thermal factors for $K(VO_2)_3(PO_3CH_3)_2$ and $NH_4(VO_2)_3(PO_3CH_3)_2$ (1 page). Ordering information is given on any current masthead page.

IC951170T

(23) Burdett, J. K. *Molecular Shapes*; Wiley-Interscience: New York, 1980.
(24) Kunz, M.; Brown, I. D. *J. Solid State Chem.* **1995**, *115*, 395.
(25) Kahn, M. I.; Lee, Y.-S.; O'Connor, C. J.; Haushalter, R. C.; Zubieta, J. *Chem. Mater.* **1994**, *6*, 721.
(26) Kahn, M. I.; Lee, Y.-S.; O'Connor, C. J.; Haushalter, R. C.; Zubieta, J. *J. Am. Chem. Soc.* **1994**, *116*, 4525.